Heterodinuclear Zinc(II)−Iron(III) Complexes and Dinuclear Zinc Complexes as Models for Zinc-Containing Phosphatases

Sabine Albedyhl,[a] David Schnieders,[a] Attila Jancsó,[b] Tamás Gajda,*[b] and Bernt Krebs*[a]

Keywords: Heterometallic complexes / Asymmetric ligands / Phosphates / Dinucleating ligands / Enzyme models

Five new dinuclear model complexes for zinc-containing phosphatases with dinucleating ligands have been prepared and characterized by single-crystal X-ray crystallography. The heterodinuclear, μ-alkoxo-bridged zinc(II)–iron(III) complexes **1**–**3** contain the symmetric ligands *N*,*N*,*N*′,*N*′-tetrakis[2-(5,6-dimethyl)benzimidazolylmethyl]-1,3-diamino-2-propanol (Htdmbpo) and *N*,*N*,*N*′,*N*′-tetrakis{2-[*N*′′-(2-hydroxyethyl)]benzimidazolylmethyl}-1,3-diamino-2-propanol (Hthebpo), and the asymmetric ligand *N*,*N*-bis[2-(4,5-dimethyl)benzimidazolylmethyl]-*N*′,*N*′-bis(2-pyridylmethyl)-1,3-diamino-2-propanol (Hbdmbbppo), respectively. X-ray crystallography revealed that the zinc center exhibits a trigonal-bipyramidal coordination, while the octahedral coordination sphere of the iron center is completed by a solvent molecule. In contrast, the zinc complexes **4** and **5**, which also have (alkoxo)(cacodylato)dimetal cores with the dinucleating ligands used in **1** and **3**, exhibit both metal centers in a trigonal-bipyramidal environment. Additionally, the solution speciation of the zinc(II) complexes formed with Htdmbpo and Hbdmbbppo were determined and the activity of the in situ prepared zinc complexes towards the transesterification of the RNA model substrate 2-(hydroxypropyl)-4-nitrophenyl phosphate (hpnp) was investigated. The dinuclear $[Zn_2LH_{-1}(OH)]^{2+}$ complex of both ligands efficiently promotes the transesterification. The kinetic data indicated a higher activity for the complex of the asymmetric ligand Hbdmbbppo, as a result of its stronger substrate binding ability.

Introduction

Model compounds simulate the characteristic properties of the active sites in enzymes. The synthesis and characterization of structural and functional model complexes contribute to the structure clarification and the comprehension of the catalytic mechanism of metalloenzymes. Investigation of inhibitor complexes and product complexes gives insight into the coordination mode of the substrate.

In this work we focused on the preparation of dinuclear model complexes for zinc-containing phosphatases. The purple acid phosphatase isolated from plants, and the serine/threonine protein phosphatase 1 and 2B (calcineurine) contain a zinc(II)−iron(III) center in their active sites.[1−3] Purple acid phosphatases hydrolyze activated phosphate monoesters within a pH range of 4−7. The octahedrally coordinated metal centers are 3.26 Å apart, and a terminal hydroxide ion at the iron center, a water molecule at the zinc center and a bridging hydroxide ion, in addition to the bridging carboxylate group of aspartate were included into the X-ray structure analysis from spectroscopic data.[1] The coordination sphere of the metal ions, which are separated by 3.3 Å and 3.0 Å, in the serine/threonine protein phosphatases 1 and 2B, respectively, is square-pyramidal at the iron atom and trigonal-bipyramidal at the zinc atom.[2] A water molecule is coordinated to the iron center, while another water molecule bridges the two metal ions. The coordination number is increased to six due to the bidentate binding of the phosphate group to the metal centers.[3]

Alkaline phosphatase, phospholipase C, nuclease P1 and phosphotriesterase contain at least two zinc centers.[4−7] Alkaline phosphatase is a widely distributed nonspecific phosphomonoesterase, which catalyzes through a covalent phosphoseryl intermediate.[8] The active site contains two zinc ions at a distance of 4.0 Å, and one magnesium ion. According to recent publications, all three metal centers contribute to the mechanism.[4] The zinc centers with a N_2O_3 donor set in the dinuclear unit of phospholipase C and nuclease P1 are bridged by a hydroxide ion or a water molecule and the carboxylate group of aspartate, and exhibit a trigonal pyramidal coordination.[5,6] Their distance apart was shown to be 3.3 Å and 3.2 Å, respectively. The bridging

[a] Anorganisch-Chemisches Institut, Westfälische Wilhelms-Universität Münster,
Wilhelm-Klemm-Straße 8, 48149 Münster, Germany
Fax: (internat.) + 49-(0)251/83-38366
E-mail: krebs@uni-muenster.de
[b] Department of Inorganic and Analytical Chemistry, University of Szeged,
P. O. Box 440, 6701 Szeged, Hungary
Fax: (internat.) + 36-(0)62/420-505
E-mail: tamas.gajda@chem.u-szeged.hu

Supporting information for this article is available on the WWW under http://www.eurjic.com or from the author.

hydroxide ion is proposed to be the attacking nucleophile in the serine/threonine protein phosphatases 1 and 2B, nuclease P1 and phosphotriesterase.

In these enzymes the first coordination sphere of the metal centers is comprised of nitrogen and oxygen donor atoms that are in common with the ligands in our systems. Furthermore, the metal−metal distances in both the enzymes and the prepared complexes are in the range of 3.0 to 4.0 Å, which is important for the co-operative interaction.

There are some examples of crystallized model compounds with interesting features reported in the literature. The model complex $[Zn_2(bbap)(Bz)(H_2O)](ClO_4)_2 \cdot 4MeOH$ {Hbbap = 2,6-bis[bis(2-benzimidazolylmethyl)aminomethyl]-4-methylphenol} for phospholipase C contains two zinc ions with different coordination spheres.[9] A new structural and perhaps functional feature in the chemistry of oligozinc enzymes was detected in the X-ray structure of $[Zn_2L(H_2O)(OH)](BPh_4)_2 \cdot 2.5C_3H_6O$ {HL = 2,5-bis[*N*,*N*-(diethylaminoethyl)aminomethyl]pyrazol}, which includes an intramolecular $H_3O_2^-$ bridge.[10] The hydrolytic activity of the complex $[Zn_2(bpan)(\mu\text{-}OH)(\mu\text{-}O_2PPh_2](ClO_4)_2$ {bpan = 2,7-bis[2-(2-pyridylethyl)aminomethyl]-1,8-naphthyridin}, in which the naphthyridin simulates the *syn*,-*syn* coordination of a bridging carboxylate group, was investigated using different model substrates.[11,12]

Currently, there is interest in the development of new ligands, especially asymmetric ligands and their metal complexes, which may be used as enzymatic models.[13−20] In addition to complexes with dissimilar metal centers due to asymmetric coordination as found in enzymes, heterodinuclear complexes are important with respect to enzymes containing two different metal ions.[21] So far, only a few heterodinuclear zinc(II)−iron(III) complexes with symmetric dinucleating ligands are known. They include four pyridine groups and contain a μ-phenoxo bridge and two further bridging ligands like acetate, diphenyl phosphate or molybdate.[22−26] Suzuki and co-workers characterized mixed-valent (μ-alkoxo)diiron(II,III) complexes with the ligand *N*,*N*,*N*′,*N*′-tetrakis(2-pyridylmethyl)-1,4-diamino-2-butanol by X-ray crystallography.[27] The asymmetric bridging unit leads to five- and six-membered chelate rings.

Here, we report on the synthesis and characterization of three heterodinuclear zinc(II)−iron(III) complexes with distinct coordination spheres, μ-alkoxo-bridging symmetric and asymmetric dinucleating ligands, as well as two corresponding zinc complexes. Their structures were determined by X-ray crystallography and characterized by additional spectroscopic measurements.

In the complexes $[Zn^{II}Fe^{III}(tdmbpo)(O_2AsMe_2)(HOMe)](ClO_4)_3 \cdot 4MeOH \cdot 2H_2O$ (**1**), $[Zn^{II}Fe^{III}(thebpo)(O_2AsMe_2)(H_2O)](ClO_4)(NO_3)_2 \cdot 3H_2O$ (**2**) and $[Zn^{II}Fe^{III}(bdmbbppo)(O_2AsMe_2)(HOMe)](ClO_4)_3 \cdot 1.5MeOH$ (**3**) the zinc ion exhibits a trigonal-bipyramidal environment, and the octahedrally ligated iron center has a coordination site occupied by a solvent molecule. This terminal solvent molecule at the iron center may act as the attacking nucleophile. In contrast to the μ-phenoxo-bridged complexes,[22−26] which are doubly bridged by two further ligands, the complexes described here contain only one further μ-cacodylato bridge. These complexes are model compounds for the kidney bean purple acid phosphatase product complex with inorganic phosphate, and for the inhibitor complex with tungstate.[1]

The zinc ions in the complexes **4** and **5** formulated as $[Zn^{II}_2(tdmbpo)(O_2AsMe_2)](ClO_4)_2 \cdot 5MeOH$ and $[Zn^{II}_2(bdmbbppo)(O_2AsMe_2)](ClO_4)_2 \cdot H_2O$, respectively, have an N_3O_2 donor set. Both zinc centers in **4** and one zinc center in **5** is symmetrically coordinated by two 4,5-dimethylbenzimidazole groups, while the second zinc center in **5** is coordinated by two pyridine groups, resulting in an asymmetric complex.

The activity of the in situ prepared complexes of these ligands and zinc perchlorate was studied with respect to the transesterification of hpnp, in order to determine the influence of the different coordinating groups. Similar systems were used by Komiyama and co-workers who investigated the cleavage of ribonucleotide dimers and compared the activity between mono-, di- and trinuclear complexes. The latter is a model for trinuclear zinc-containing phosphodiesterases like phospholipase C and nuclease P1.[28,29] Very efficient di- and trinuclear zinc catalysts, which were also prepared in situ, were described by Engbersen, Reinhoudt and co-workers and are based on calix[4]arene.[30−33] Recently, zinc-containing complexes with dinucleating imidazole ligands have been studied.[34,35] As various types of mechanisms are discussed, particularly with regards to the reacting nucleophile and the coordination mode of the substrate, further information will be drawn from the study of model complexes. Important aspects are the determination of the crystal structure, the identification of the active species in solution and the mechanism of the reaction of model compounds with substrates.

Results and Discussion

X-ray Crystal Structures of 1, 2 and 3

In order to mimic the active site of kidney bean purple acid phosphatase we used the symmetric and asymmetric dinucleating ligands Htdmbpo, Hthebpo and Hbdmbbppo to form heterodinuclear μ-alkoxo-bridged zinc(II)−iron(III) complexes with two differently coordinated metal centers. The zinc ion has a trigonal-bipyramidal geometry with an N_3O_2 donor set, whereas the iron center resides in an octahedral environment that is completed by a solvent ligand. Structures of the cations in **1**, **2** and **3** are depicted in Figures 1, 2 and 3.

The zinc ions are facially coordinated by two benzimidazole nitrogen atoms (N3 and N5) and one tertiary aliphatic nitrogen atom (N1) of the ligand. The iron centers in **1** and **2** are also coordinated by two benzimidazole nitrogen atoms (N7 and N9) and one tertiary aliphatic nitrogen atom (N2) of the ligand. The iron center in **3** is facially ligated by two pyridine nitrogen atoms (N7 and N8) and one tertiary aliphatic nitrogen atom (N2) of the ligand bdmbbppo. The metal centers are connected by the deprotonated μ-alkoxo

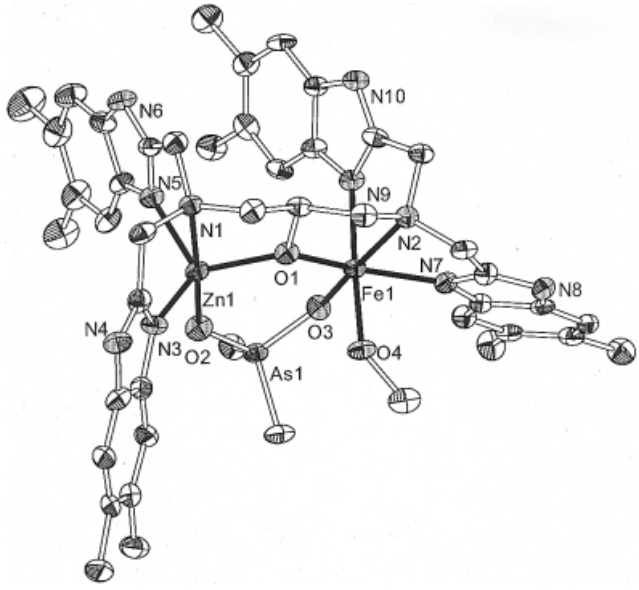

Figure 1. Structure of the cation in **1** showing 50% probability displacement ellipsoids; hydrogen atoms have been omitted for clarity

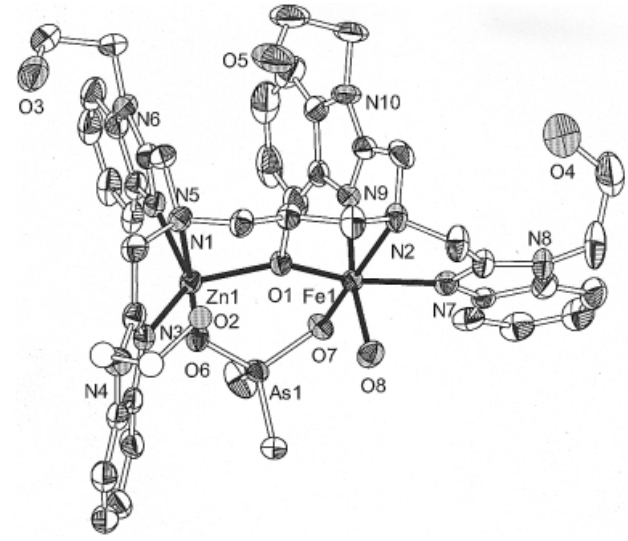

Figure 2. Structure of the cation in **2** showing 50% probability displacement ellipsoids; one hydroxyethyl group was refined isotropically; hydrogen atoms have been omitted for clarity

oxygen atom O1 of the ligand and the cacodylate bridge. An N_3O_3 donor set of the iron(III) center is formed by the additional coordination of a methanol molecule (O4−C46 and O4−C38) in **1** and **3**, respectively, and by a water molecule (O8) in **2**. The coordination polyhedra share one edge (O1). The cacodylate bridge in the inhibitor complexes shows the same bridging mode as in the enzyme. The inter-metal distances in **1**, **2** and **3** are 3.5635(12), 3.6053(13) and 3.5354(12) Å, respectively, and are slightly larger than in the enzyme. The Zn1−O1−Fe1 angles are 125.9(2)° in **1**, 127.7(2)° in **2** and 125.3(3)° in **3** and follow the same trend observed for the inter-metal distances (Table 1).

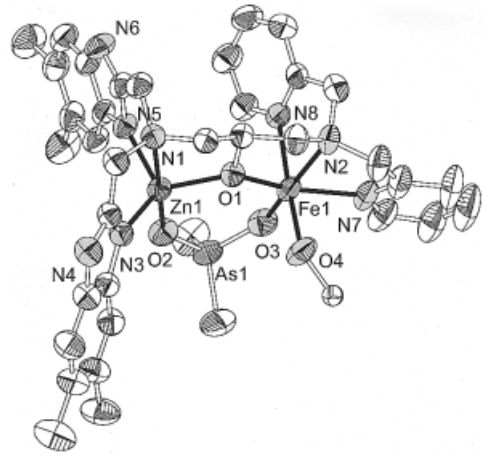

Figure 3. Structure of the cation in **3** showing 50% probability displacement ellipsoids

The axial positions of the trigonal-bipyramidal coordination polyhedra of the zinc ions are occupied by the tertiary nitrogen atom N1 and the oxygen atom of the cacodylate group, O2 in **1** and **3** and O6 in **2**. The distortion of the ideal coordination polyhedra towards the tertiary nitrogen atom results in angles smaller than 90° between N1 and the equatorially bound donor atoms. The geometrical distortion around the iron centers is demonstrated by the deviation of the three angles of the axial donor atoms by about 16° from the ideal 180° angle. The coordination polyhedra of the iron centers are distorted towards the tertiary nitrogen atom N2 in a similar manner as in the zinc centers. The angles between N2 and the atoms in *cis* position O1, N7 and N9 (N8 in **3**) are smaller than 90°, while the angles between N2 and the oxygen atoms O4 of the bound methanol molecules and the oxygen atom O8 of the water molecule are close to 90°.

The bond lengths between the tertiary nitrogen atoms (N1, N2) and the metal ions are much larger than the bond lengths between the aromatic nitrogen atoms of the ligands and the metal ions (Table 2). The bonds between Fe1 and the oxygen atoms O4 of the coordinating methanol molecules in **1** and **3** have lengths of 2.172(4) and 2.054(4) Å, respectively, as a result of the different properties of the benzimidazole and pyridine groups coordinated to the iron centers. The bond lengths between the oxygen atom O8 of the coordinating water molecule and Fe1 in **2** is 2.068(4) Å. The hydroxide ion coordinated to the iron(III) center has a much smaller distance of about 1.90 Å.[36]

To date, only the μ-cacodylato-bridged dinuclear complexes $[Fe^{III}_2(tbpo)(O_2AsMe_2)(OMe)(HOMe)](ClO_4)_3 \cdot 5MeOH \cdot 2H_2O$[37] [Htbpo = *N*,*N*,*N*′,*N*′-tetrakis(2-benzimidazolylmethyl)-1,3-diamino-2-propanol], $[Fe^{III}_2(tbpo)(O_2AsMe_2)(Cl)(H_2O)](ClO_4)_3 \cdot 5MeOH \cdot H_2O$[38] and $[Fe^{III}_2(mtbpo)(O_2AsMe_2)(Cl)_2(HOMe)](ClO_4)_2 \cdot 4MeOH$[39] [Hmtbpo = *N*,*N*,*N*′-tris(2-benzimidazolylmethyl)-*N*′-methyl-1,3-diamino-2-propanol] are known in which both iron centers have an octahedral coordination sphere. The distance between the oxygen atom of the water molecule and the iron(III) center in the second complex is 2.088(6)

Table 1. Selected angles [°] in **1**, **2** and **3**

1		**2**		**3**	
Zn(1)−O(1)−Fe(1)	125.9(2)	Zn(1)−O(1)−Fe(1)	127.7(2)	Zn(1)−O(1)−Fe(1)	125.3(3)
O(1)−Zn(1)−O(2)	104.0(2)	O(1)−Zn(1)−O(6)	101.9(2)	O(1)−Zn(1)−O(2)	102.6(2)
O(1)−Zn(1)−N(1)	78.4(2)	O(1)−Zn(1)−N(1)	79.6(2)	O(1)−Zn(1)−N(1)	78.3(1)
O(1)−Zn(1)−N(3)	116.0(2)	O(1)−Zn(1)−N(3)	117.4(2)	O(1)−Zn(1)−N(3)	118.0(2)
O(1)−Zn(1)−N(5)	112.6(2)	O(1)−Zn(1)−N(5)	106.9(2)	O(1)−Zn(1)−N(5)	109.8(2)
O(2)−Zn(1)−N(1)	177.0(2)	O(6)−Zn(1)−N(1)	176.4(2)	O(2)−Zn(1)−N(1)	178.9(2)
O(2)−Zn(1)−N(3)	99.6(2)	O(6)−Zn(1)−N(3)	99.8(2)	O(2)−Zn(1)−N(3)	102.1(2)
O(2)−Zn(1)−N(5)	104.9(2)	O(6)−Zn(1)−N(5)	105.8(2)	O(2)−Zn(1)−N(5)	105.2(2)
N(1)−Zn(1)−N(3)	77.7(2)	N(1)−Zn(1)−N(3)	76.7(2)	N(1)−Zn(1)−N(3)	76.9(2)
N(1)−Zn(1)−N(5)	75.5(2)	N(1)−Zn(1)−N(5)	76.7(2)	N(1)−Zn(1)−N(5)	75.1(2)
N(3)−Zn(1)−N(5)	117.1(2)	N(3)−Zn(1)−N(5)	122.1(2)	N(3)−Zn(1)−N(5)	116.9(2)
O(1)−Fe(1)−O(3)	104.5(2)	O(1)−Fe(1)−O(7)	104.2(2)	O(1)−Fe(1)−O(3)	107.6(2)
O(1)−Fe(1)−O(4)	80.8(2)	O(1)−Fe(1)−O(8)	88.0(2)	O(1)−Fe(1)−O(4)	86.5(2)
O(1)−Fe(1)−N(2)	81.2(2)	O(1)−Fe(1)−N(2)	80.2(2)	O(1)−Fe(1)−N(2)	81.7(2)
O(1)−Fe(1)−N(7)	152.7(2)	O(1)−Fe(1)−N(7)	154.1(2)	O(1)−Fe(1)−N(7)	155.8(2)
O(1)−Fe(1)−N(9)	92.1(2)	O(1)−Fe(1)−N(9)	93.1(2)	O(1)−Fe(1)−N(8)	87.8(2)
O(3)−Fe(1)−O(4)	96.2(2)	O(7)−Fe(1)−O(8)	96.8(2)	O(3)−Fe(1)−O(4)	97.9(2)
O(3)−Fe(1)−N(2)	173.4(2)	O(7)−Fe(1)−N(2)	173.5(2)	O(3)−Fe(1)−N(2)	167.1(2)
O(3)−Fe(1)−N(7)	100.3(2)	O(7)−Fe(1)−N(7)	101.3(2)	O(3)−Fe(1)−N(7)	96.1(2)
O(3)−Fe(1)−N(9)	97.4(2)	O(7)−Fe(1)−N(9)	96.3(2)	O(3)−Fe(1)−N(8)	93.2(2)
O(4)−Fe(1)−N(2)	87.8(2)	O(8)−Fe(1)−N(2)	88.1(2)	O(4)−Fe(1)−N(2)	91.5(2)
O(4)−Fe(1)−N(7)	85.5(2)	O(8)−Fe(1)−N(7)	84.2(2)	O(4)−Fe(1)−N(7)	85.5(2)
O(4)−Fe(1)−N(9)	165.9(2)	O(8)−Fe(1)−N(9)	166.2(2)	O(4)−Fe(1)−N(8)	168.6(3)
N(2)−Fe(1)−N(7)	74.8(2)	N(2)−Fe(1)−N(7)	74.9(2)	N(2)−Fe(1)−N(7)	75.8(2)
N(2)−Fe(1)−N(9)	79.0(2)	N(2)−Fe(1)−N(9)	78.6(2)	N(2)−Fe(1)−N(8)	77.9(2)
N(7)−Fe(1)−N(9)	95.8(2)	N(7)−Fe(1)−N(9)	89.0(2)	N(7)−Fe(1)−N(8)	95.7(2)

Table 2. Selected bond lengths [Å] in **1**, **2** and **3**

1		**2**		**3**	
Zn(1)···Fe(1)	3.5635(12)	Zn(1)···Fe(1)	3.6053(13)	Zn(1)···Fe(1)	3.5354(12)
Zn(1)−O(1)	2.035(4)	Zn(1)−O(1)	2.049(4)	Zn(1)−O(1)	2.024(3)
Zn(1)−O(2)	1.978(4)	Zn(1)−O(6)	1.955(4)	Zn(1)−O(2)	1.964(4)
Zn(1)−N(1)	2.406(4)	Zn(1)−N(1)	2.385(5)	Zn(1)−N(1)	2.448(4)
Zn(1)−N(3)	2.012(5)	Zn(1)−N(3)	2.034(5)	Zn(1)−N(3)	2.009(4)
Zn(1)−N(5)	2.017(4)	Zn(1)−N(5)	2.011(5)	Zn(1)−N(5)	2.002(4)
Fe(1)−O(1)	1.967(4)	Fe(1)−O(1)	1.967(4)	Fe(1)−O(1)	1.956(4)
Fe(1)−O(3)	1.880(4)	Fe(1)−O(7)	1.874(4)	Fe(1)−O(3)	1.871(4)
Fe(1)−O(4)	2.172(4)	Fe(1)−O(8)	2.068(4)	Fe(1)−O(4)	2.054(4)
Fe(1)−N(2)	2.283(4)	Fe(1)−N(2)	2.283(5)	Fe(1)−N(2)	2.203(5)
Fe(1)−N(7)	2.073(4)	Fe(1)−N(7)	2.103(5)	Fe(1)−N(7)	2.137(4)
Fe(1)−N(9)	2.075(4)	Fe(1)−N(9)	2.074(5)	Fe(1)−N(8)	2.147(4)

Å, and therefore is similar to the corresponding distance in **2**. The presence of only one iron(III) center in both complexes was confirmed by magnetic measurements, where a linear increase of $1/\chi$ with temperature and no coupling effects were observed. The experimental μ_{eff} values are in accordance with the theoretical value of 5.92 μ_B for a high-spin iron(III) ion.

X-ray Crystal Structures of 4 and 5

The structures of the cations in **4** and **5** are provided in the Supporting Information (Figures S1 and S2).

The metal centers in complexes **4** and **5** have a trigonal-bipyramidal coordination sphere, with an N_3O_2 donor set. Their inter-metal distances are 3.562(2) Å and 3.5147(16) Å, respectively. Each zinc ion is facially coordinated by two benzimidazole nitrogen atoms (N3, N5 and N7, N9) or two pyridine nitrogen atoms (N7 and N8) and one tertiary aliphatic nitrogen atom (N1 or N2) of the ligand. They are connected by the deprotonated μ-alkoxo oxygen atom O1 of the ligand and one cacodylate bridge. The coordination polyhedra share one edge (O1). The Zn1−O1−Zn2 angles are 128.0(4)° and 125.9(3)°, respectively (Table 3). The axial positions of the trigonal-bipyramidal coordination polyhedra of the zinc ions are occupied by the tertiary nitrogen atoms N1 or N2, and one oxygen atom O2 or O3 of the cacodylate bridge. The average deviation from 180° is 2.3° at one metal center and 8.7° at the other metal center. The coordination polyhedra are distorted towards the tertiary nitrogen atoms as observed at the zinc centers in the complexes **1**, **2** and **3**. The differences in the average values for

Table 3. Selected angles [°] in **4** and **5**

4		**5**	
Zn(1)−O(1)−Zn(2)	128.0(4)	Zn(1)−O(1)−Zn(2)	125.9(3)
O(1)−Zn(1)−O(2)	101.5(3)	O(1)−Zn(1)−O(2)	103.6(3)
O(1)−Zn(1)−N(1)	78.6(3)	O(1)−Zn(1)−N(1)	78.8(3)
O(1)−Zn(1)−N(3)	117.8(4)	O(1)−Zn(1)−N(3)	114.9(3)
O(1)−Zn(1)−N(5)	118.4(4)	O(1)−Zn(1)−N(5)	121.6(3)
O(2)−Zn(1)−N(1)	178.0(4)	O(2)−Zn(1)−N(1)	177.5(3)
O(2)−Zn(1)−N(3)	105.8(4)	O(2)−Zn(1)−N(3)	103.2(3)
O(2)−Zn(1)−N(5)	102.2(4)	O(2)−Zn(1)−N(5)	102.9(3)
N(1)−Zn(1)−N(3)	75.9(4)	N(1)−Zn(1)−N(3)	75.5(3)
N(1)−Zn(1)−N(5)	76.0(4)	N(1)−Zn(1)−N(5)	75.6(3)
N(3)−Zn(1)−N(5)	108.7(4)	N(3)−Zn(1)−N(5)	108.1(3)
O(1)−Zn(2)−O(3)	106.2(3)	O(1)−Zn(2)−O(3)	107.2(3)
O(1)−Zn(2)−N(2)	81.7(3)	O(1)−Zn(2)−N(2)	82.2(3)
O(1)−Zn(2)−N(7)	111.2(4)	O(1)−Zn(2)−N(7)	115.7(3)
O(1)−Zn(2)−N(9)	109.7(4)	O(1)−Zn(2)−N(8)	113.8(3)
O(3)−Zn(2)−N(2)	172.1(3)	O(3)−Zn(2)−N(2)	170.5(3)
O(3)−Zn(2)−N(7)	103.3(4)	O(3)−Zn(2)−N(7)	99.5(4)
O(3)−Zn(2)−N(9)	100.3(3)	O(3)−Zn(2)−N(8)	96.6(3)
N(2)−Zn(2)−N(7)	73.6(4)	N(2)−Zn(2)−N(7)	77.2(4)
N(2)−Zn(2)−N(9)	76.2(3)	N(2)−Zn(2)−N(8)	77.7(3)
N(7)−Zn(2)−N(9)	124.0(4)	N(7)−Zn(2)−N(8)	119.8(3)
O(2)−As(1)−O(3)	112.8(4)	O(2)−As(1)−O(3)	114.0(3)

the angles between the tertiary nitrogen atoms and the equatorially bound donor atoms of 76.8 and 77.2° in **4** and 76.6 and 79.0° in **5**, result from different coordinating groups at each metal center.

In addition, the bond lengths between the tertiary nitrogen atoms and the metal ions are longer than the bond lengths between the aromatic nitrogen atoms of the ligands and the metal ions (Table 4). The distances between the tertiary nitrogen atoms and the zinc ions are 2.375(9) Å and 2.387 (8) Å in **4**, and 2.467(7) Å and 2.255(8) Å in **5**. The greater difference (0.212 Å) between the distances observed in **5** is due to the asymmetry in complex **5**.

Table 4. Selected bond lengths [Å] in **4** and **5**

4		**5**	
Zn(1)···Zn(2)	3.562(2)	Zn(1)···Zn(2)	3.5147(16)
Zn(1)−O(1)	1.993(7)	Zn(1)−O(1)	1.980(7)
Zn(1)−O(2)	1.950(7)	Zn(1)−O(2)	1.953(6)
Zn(1)−N(1)	2.375(9)	Zn(1)−N(1)	2.467(7)
Zn(1)−N(3)	2.051(10)	Zn(1)−N(3)	2.015(8)
Zn(1)−N(5)	1.982(10)	Zn(1)−N(5)	2.024(10)
Zn(2)−O(1)	1.970(7)	Zn(2)−O(1)	1.966(7)
Zn(2)−O(3)	1.998(7)	Zn(2)−O(3)	1.955(6)
Zn(2)−N(2)	2.387(8)	Zn(2)−N(2)	2.255(8)
Zn(2)−N(7)	1.997(12)	Zn(2)−N(7)	2.094(10)
Zn(2)−N(9)	2.066(9)	Zn(2)−N(8)	2.068(8)

Solution Speciation

The solubility of the ligands and complexes in an ethanol/water mixed solvent allowed the solution study of the zinc(II) complexes of Htdmbpo (in 80 % ethanol/water, w/w) and Hbdmbbppo (in 35 % ethanol/water, w/w). These studies involved a series of pH-dependent measurements.

Table 5. Logarithmic formation constants for the proton and zinc(II) complexes of Htdmbpo (in 80 % ethanol/water, w/w, T = 298 K, I = 0.05 M $NaNO_3$) and of Hbdmbbppo (in 35 % ethanol/water, w/w , T = 298 K, I = 0.1 M $NaNO_3$); $\beta_{pqr} = [M_pL_qH_K]/[M]^p[L]^q[H]^r$, with estimated errors in parentheses (last digit)

pqr	β_{pqr} Htdmbpo	β_{pqr} Hbdmbbppo
011	5.91(2)	6.01(1)
012	10.54(2)	10.96(1)
013	14.35(2)	14.93(2)
014	16.71(2)	17.93(2)
112	−	16.37(4)
111	12.74(4)	12.47(8)
110	10.65(2)	9.80(3)
21−1	10.87(3)	9.56(4)
21−2	3.80(4)	2.43(5)
21−3	−4.00(5)	−6.90(5)
pK_{21-2}^{21-1}	7.07	7.13
pK_{21-3}^{21-2}	7.80	9.33
NP[a] (FP[b])	283 (0.012 cm^{-3})	300 (0.010 cm^{-3})

[a] NP: number of experimental points. [b] FP: fitting parameter.

The determined protonation and complex formation constants are listed in Table 5, together with some derived data (see pH-metric measurements in the Exp. Sect.). Four strongly overlapping deprotonation processes were observed at pH > 2 for both ligands. The fifth and sixth pK values are therefore much lower than 2, presumably due to the formation of a hydrogen bond between the two substituents of a given tertiary amino group.

In the presence of zinc(II) the same species were formed with both ligands. In an equimolar solution, the complex $[ZnL]^{2+}$ is dominant in the neutral pH range. Dinuclear $[Zn_2LH_{-x}]^{(4-x)+}$ complexes (x = 1−3) are also formed at pH > 7. The latter species already becomes dominant at pH = 4, in the presence of a twofold metal excess (Figure 4). The deprotonation during the formation of the first dinuclear complex ($[ZnL]^{2+} + Zn^{2+} = [Zn_2LH_{-1}]^{3+} + H^+$) takes place at surprisingly low pH (at pH ≈ 4), which suggests a concerted action of the two zinc(II) ions. The participation of the hydroxy group in this process should be particularly favorable, due to the preorganization of the metal ions by the ligand. In this way, the complex $[Zn_2LH_{-1}]^{3+}$ most likely has the same single μ-alkoxo-bridged structure as crystallographically determined for the complexes **4** and **5**. The succeeding two deprotonations, leading to the complexes $[Zn_2LH_{-2}]^{2+}$ and $[Zn_2LH_{-3}]^{+}$, involve the deprotonation of coordinated water molecules (the metal-induced deprotonation of the pyrrolic nitrogen atom of the benzimidazole moieties at pH ≈ 7−8, is very unlikely in the case of zinc(II)), thus they are better described as $[Zn_2LH_{-1}(OH)]^{2+}$ and $[Zn_2LH_{-1}(OH)_2]^{+}$. These two successive processes are rather well separated for the Hbdmbbppo complex ($pK_2 - pK_1 = \Delta pK$ = 2.2, see Table 5), which allows the formation of the species M_2LH_{-2} in relatively high concentrations, while ΔpK is only 0.73 for the Htdmbpo complex. The solution speciation of these systems is clearly different from that observed for a *N*,*N*′-dis-

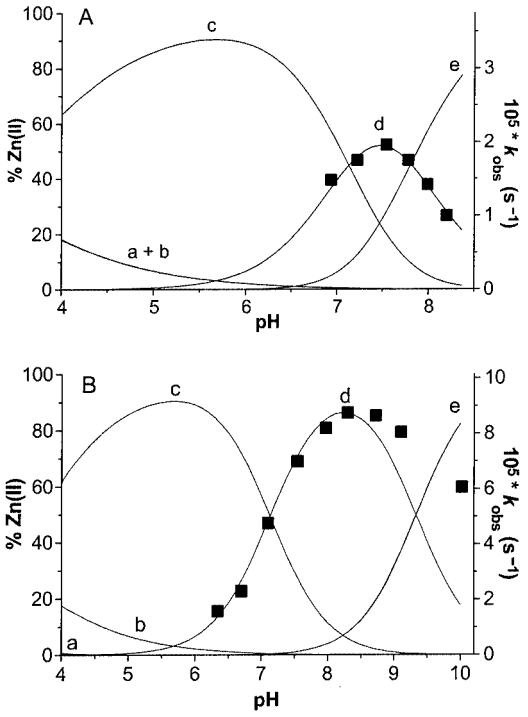

Figure 4. Species distribution curves (solid lines) and the effect of pH on the transesterification of hpnp (filled square) for the zinc(II)−Htdmbpo (A) and −Hbdmbbppo (B) systems (T = 298 K, [Htdmbpo] = 0.4 mM, [Hbdmbbppo] = 0.8 mM, $[Zn^{II}]/[L]$ = 2:1, [hpnp] = 1 mM); a: Zn^{II}, b: $[ZnL]^{2+}$, c: $[Zn_2LH_{-1}]^{3+}$, d: $[Zn_2LH_{-1}(OH)]^{2+}$, e: $[ZnLH_{-1}(OH)_2]^{+}$

ubstituted imidazole derivative of 1,3-diamino-2-propanol (in 65 % ethanol/water, w/w mixture)[34], where the process $[ZnL]^{2+} + Zn^{2+} = [Zn_2LH_{-1}(OH)]^{2+} + 2\ H^{+}$ takes place in a single step. This difference is probably the result of the higher stabilization of the 3*N*-coordinated zinc(II) ions in the present case. This can be demonstrated by the log *K* values of the above process, which are −7.06 for Htdmbpo, −7.37 for Hbdmbbppo and −11.34 for the *N*,*N*′-disubstituted imidazole derivative.[34]

Hydrolytic Studies

To screen the hydrolytic activity of the two systems described above, their ability to promote the transesterification of 2-(hydroxypropyl)-4-nitrophenyl phosphate (hpnp) was investigated. For these purposes pH-dependent measurements were carried out (see Exp. Sect.). In both the zinc(II)−Htdmbpo and −Hbdmbbppo ($[Zn^{II}]/[L]$ = 2:1) systems, notable transesterification activity was observed at pH > 6, parallel with the formation of the dinuclear species $Zn_2LH_{-1}(OH)$ (Figure 4). Based on the pH/rate constant profile, the successively formed $Zn_2LH_{-1}(OH)_2$ complex of Hbdmbbppo is also able to promote the transesterification, and its activity is almost half of the former $Zn_2LH_{-1}(OH)$ species. Such behavior was not observed with Htdmbpo. This difference may in part be due to the presence of the four bulky benzimidazole residues in Htdmbpo, which lower the binding ability of hpnp to the metal centers.

The rate of the transesterification shows first-order dependence on the concentration of the dinuclear complex

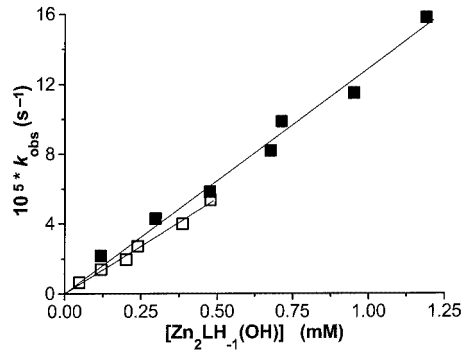

Figure 5. Dependence of k_{obs} on the concentration of $[Zn_2LH_{-1}(OH)]^{2+}$ complex of Htdmbpo (open square, pH = 7.50) and Hbdmbbppo (filled square, pH = 8.00); T = 298 K, $[Zn^{II}]/[L]$ = 2:1, [hpnp] = 1 mM

$[Zn_2LH_{-1}(OH)]^{2+}$ (Figure 5). The second-order rate constants determined from these plots are 0.109(3) $M^{-1}s^{-1}$ for Htdmbpo, and 0.129(4) $M^{-1}s^{-1}$ for Hbdmbbppo. These constants are somewhat higher than the second-order rate constant for the hydroxide ion catalyzed reaction (k_{OH} = 0.0745 $M^{-1}s^{-1}$).[34]

The initial rate of transesterification has also been determined as a function of the substrate concentration. The data depicted in Figure 6 show substrate saturation above 40−80-fold excess of hpnp. This indicates the validity of the Michaelis−Menten kinetics in our systems, i.e. the formation of a ternary $[Zn_2LH_{-1}(OH)(hpnp)]^{+}$ complex prior to the intramolecular transformation. The nonlinear least-squares fit of the data points, solid lines in Figure 6, gave the Michaelis constants (K_M) 12.9 mM and 5.2 mM, and catalytic rate constants (k_{cat}) 1.10×10^{-3} s^{-1} and 8.33×10^{-4} s^{-1} for the $[Zn_2LH_{-1}(OH)]^{2+}$ complexes of Htdmbpo and Hbdmbbppo, respectively. These k_{cat} values indicate ca. four orders of magnitude maximal rate acceleration for the hpnp transesterification by these complexes.[34] The dinuclear Htdmbpo zinc(II) complex possesses a somewhat higher catalytic rate constant, but its substrate binding ($1/K_M$) is two and a half times less effective than that of the corresponding Hbdmbbppo complex, which results in a higher overall activity of the latter complex.

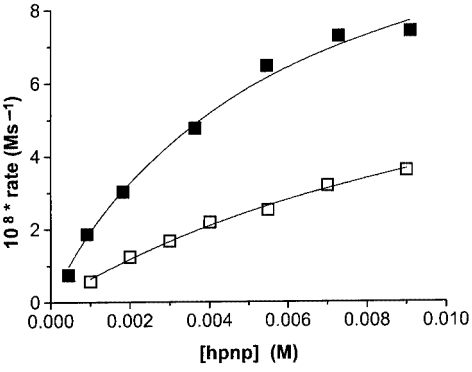

Figure 6. Saturation kinetic experiments for the transesterification of hpnp by the zinc(II)−Htdmpbo (open square, pH = 7.50, [L] = 1.6×10^{-4} M) and the zinc(II)−Hbdmbbppo (filled square, pH = 7.90, [L] = 1.8×10^{-4} M) systems; T = 298 K, $[Zn^{II}]/[L]$ = 2:1

By analogy with the crystal structure of complexes **4** and **5** (which contain the cacodylate bridging unit analogous to the phosphate), $\mu_{1,3}$-bridged coordination of the substrate hpnp can be envisaged for the dinuclear center. This would create a double Lewis acid activation for the transesterification reaction. However, the inactivity of the species $[Zn_2LH_{-1}]^{3+}$ (Figure 4), clearly demonstrates that this effect alone does not provide sufficient rate acceleration. This would need the concerted action of the double Lewis acid activation and the intramolecular general base catalysis by a metal-bound hydroxide ion, which becomes possible only in the successively formed $[Zn_2LH_{-1}(OH)]^{2+}$ complex (Scheme 1).

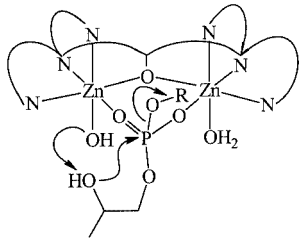

Scheme 1. The proposed mechanism for the transesterification of hpnp by the dinuclear zinc(II) complexes

Conclusion

With the syntheses of the complexes **1**, **2** and **3**, the first characterization of three structurally similar, heterodinuclear zinc(II)−iron(III) complexes with bridging μ-alkoxo units has been accomplished. According to their structural and spectroscopic properties they are excellent structural models of the active site of kidney bean purple acid phosphatase, serine/threonine protein phosphatase 1 and calcineurin. The use of an asymmetric ligand offers the possibility to prepare tailor-made heterodinuclear complexes. The trigonal-bipyramidally coordinated zinc ion and the octahedrally coordinated iron center are bridged by only one additional cacodylate ligand. The coordination of a water or a methanol molecule to the iron(III) center is very interesting with respect to the discussion of the nucleophilic species in the catalytic mechanism of kidney bean purple acid phosphatase.

The dinuclear zinc complexes **4** and **5** serve as models for alkaline phosphatase, phospholipase C, nuclease P1 and phosphotriesterase. The in situ prepared dinuclear $[Zn_2LH_{-1}(OH)]^{2+}$ complexes of Htdmbpo and Hbdmbbppo possess notable transesterification activity towards the RNA model hpnp, around the neutral pH range. The dinuclear complex formed with the asymmetric ligand Hbdmbbppo showed higher activity as compared with that of the symmetric ligand Htdmbpo, due to its higher substrate binding ability. The results suggest a bifunctional mechanism in the case of both ligands, i.e. the concerted action of the double Lewis acid activation provided by the dimetallic core and the intramolecular general base catalysis provided by a zinc(II)-bound hydroxide ion.

Experimental Section

General Remarks: All chemicals were obtained from commercial sources and used as received. ***CAUTION:*** Although no problems were encountered, suitable care and precautions should be taken when handling the perchlorate salts.

Physical Measurements: ^{1}H NMR spectra were recorded with a Bruker AC 200 instrument. The chemical shifts are reported relative to an internal standard of tetramethylsilane. Elemental analyses were performed with an elemental Vario El III instrument. IR spectra were recorded with a Bruker IFS 48 FT spectrometer. UV/Vis spectra were obtained using a UVIKON 933 spectrometer of Kontron Instruments equipped with 1.0-cm matched quartz cells and operating in the range 190−900 nm. Cyclic voltammetric measurements were carried out using a BAS CV-50 W potentiostat. All experiments were run at room temperature under argon. A standard three-electrode cell was used equipped with a platinum electrode, an Ag/AgCl/3 M NaCl reference electrode and a glassy carbon electrode. Tetra-*n*-butylammonium perchlorate (0.1 M) was used as the supporting electrolyte. Magnetic susceptibility measurements were carried out with a Quantum Design SQUID magnetometer at 3 T in a temperature range of 2−300 K. The mass spectra were recorded with an electrospray mass spectrometer Quattro LCZ with a nanospray inlet.

Synthesis: The barium salt of 2-(hydroxypropyl)-4-nitrophenyl phosphate (hpnp) was prepared according to a literature procedure.[40]

***N*,*N*,*N*′,*N*′-Tetrakis[2-(5,6-dimethyl)benzimidazolylmethyl]-1,3-diamino-2-propanol (Htdmbpo) and *N*,*N*,*N*′,*N*′-Tetrakis[2-(*N*′′-(2-hydroxyethyl)]benzimidazolylmethyl]-1,3-diamino-2-propanol (Hthebpo):** The symmetric ligands Htdmbpo and Hthebpo were synthesized as described previously.[41]

***N*,*N*-Bis[2-(4,5-dimethyl)benzimidazolylmethyl]-*N*′,*N*′-bis(2-pyridylmethyl)-1,3-diamino-2-propanol (Hbdmbbppo):** The asymmetric ligand Hbdmbbppo was prepared in a multi-step synthesis using *N*,*N*-bis(2-pyridylmethyl)-1,3-diamino-2-propanol. The preparation of the latter was carried out according to the procedure reported by Suzuki et al. with some modifications.[13] A mixture of phthalimidomethyloxirane and bis(2-pyridylmethyl)amine was heated for 3 d at 100−110 °C. The product was purified by silica gel column chromatography with a chloroform/methanol ratio of 9:1. The synthetic route of the final steps is depicted in Scheme 2.

Chloroacetic acid (2.58 g, 27 mmol) was dissolved in water (6 mL). An aqueous solution (8 mL) of sodium hydroxide (1.08 g, 35 mmol) was added under cooling in an ice bath. *N*,*N*-Bis(2-pyridylmethyl)-1,3-diamino-2-propanol (3.72 g, 14 mmol) was then added, and the mixture was heated to 65 °C. Once more an aqueous solution (8 mL) of sodium hydroxide (1.08 g, 35 mmol) was added over 1 h. After the solution had been stirred at 65 °C for 3 h, 6 M hydrochloric acid (13.6 mL, 90.9 mmol) was added. The solvent was removed in a rotary evaporator and the remaining solid was dissolved in ethanol. The precipitate was filtered off and the solvent was removed in a rotary evaporator to give *N*,*N*-bis(carboxyethyl)-*N*′,*N*′-bis(2-pyridylmethyl)-1,3-diamino-2-propanol. The product was used without further purification.

N,*N*-Bis(carboxyethyl)-*N*′,*N*′-bis(2-pyridylmethyl)-1,3-diamino-2-propanol (6.13 g, 16 mmol) and 4,5-dimethyl-1,2-phenylenediamine (4.49 g, 33 mmol) were dissolved in ethanol (5 mL) and thoroughly mixed, the solvent was subsequently removed. The mixture was heated for 3 h at 130 °C until no further water steam de-

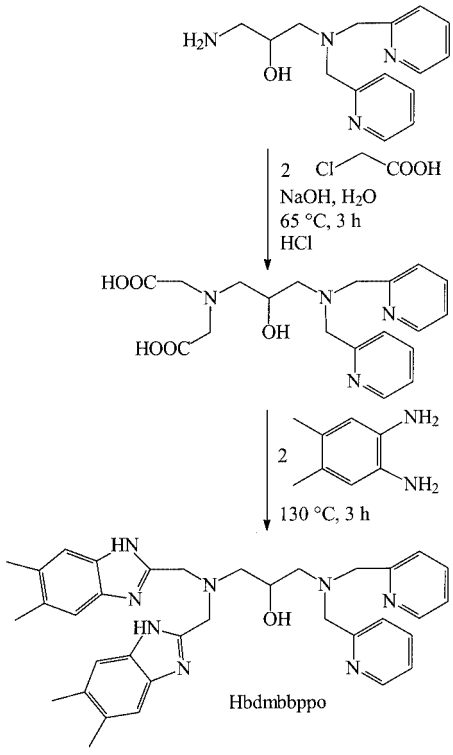

Scheme 2. Final synthetic steps in the preparation of Hbdmbbppo

veloped. The residue was dissolved in a minimum of ethanol in a sonic bath. This solution was added to a mixture of water (150 mL) and concentrated ammonia (7 mL). A brown oily product precipitated, which was purified by silica gel column chromatography with tetrahydrofuran/methanol, 3:1. Yield: 5.09 g (8 mmol, 50%). M.p. 168 °C. ^{1}H NMR (200 MHz, $CDCl_3$): δ = 2.08 (m, 4 H, CH−CH_2−N), 2.35 (s, 12 H, CH_3), 3.86 (m, 9 H, CH, N−CH_2), 7.26 (m, 10 H, Ar−H), 8.39 (d, 2 H, Ar−H). IR (KBr, 4000−400 cm^{-1}): $\tilde{\nu}$ [cm^{-1}] = 3391 (s), 3054 (w), 2922 (s), 1722 (w), 1634(w), 1593 (s), 1571 (w), 1538 (w), 1447 (s), 1364 (m), 1308 (m), 1262 (w), 1149 (w), 1121 (w), 1096 (w), 1048 (w), 1021 (w), 1001 (w), 980 (w), 858 (m), 799 (w), 764 (s), 666 (w), 630 (w), 461 (w), 436 (w). MS: *m*/*z* = 589 $[M + H]^+$.

[$Zn^{II}Fe^{III}$(tdmbpo)(O_2AsMe_2)(HOMe)](ClO_4)$_3$·4MeOH·2H_2O (1): A methanol solution (5 mL) containing $Zn(ClO_4)_2$·6H_2O (64 mg, 0.17 mmol) and $Fe(ClO_4)_3$·9H_2O (89 mg, 0.17 mmol) was added to a suspension of Htdmbpo (141 mg, 0.17 mmol) in methanol (5 mL). The sodium salt of cacodylic acid (37 mg, 0.17 mmol), dissolved in methanol (5 mL), was then added to the solution. After slow evaporation of the solvent, red orange crystals (132 mg, 0.09 mmol, 52%) were obtained after 2 d. UV/Vis (acetonitrile): λ_{max} = 402 nm (ε = 2458 $M^{-1}cm^{-1}$). $C_{50}H_{79}AsCl_3FeN_{10}O_{22}Zn$ (1474.7): calcd. C 40.72, H 5.40, N 9.50; found C 40.07, H 5.24, N 9.78. Cyclic voltammetry (250 mV/s) in acetonitrile (1 mM): $E_{1/2}$ = 99 mV (Zn^{II}−Fe^{II}/Zn^{II}−Fe^{III}). The cathodic peak at −760 mV is arsenic-centered, μ_{eff} = 5.92 μ_B.

[$Zn^{II}Fe^{III}$(thebpo) (O_2AsMe_2)(H_2O)](ClO_4)(NO_3)$_2$·3H_2O (2): An aqueous solution (2.3 mL) of $Zn(NO_3)_2$·6H_2O (45 mg, 0.15 mmol) was added to a solution of Hthebpo (137 mg, 0.15 mmol) in acetonitrile (7.5 mL). After a few minutes, an aqueous solution (2.5 mL) of $Fe(NO_3)_3$·9H_2O (61 mg, 0.15 mmol) was added dropwise. A solution of the sodium salt of cacodylic acid, dissolved in acetonitrile (2.5 mL), was added after a few minutes. The pH of the solution was determined to be 3. After a few days, orange crystals (45 mg, 0.04 mmol, 23%) suitable for X-ray crystallography were obtained by diffusion of diethyl ether into the solution. The perchlorate anion in the complex is taken from the perchlorate adduct of the ligand. $C_{45}H_{63}AsClFeN_{12}O_{21.5}Zn$ (1347.7): calcd. C 40.11, H 4.71, N 12.47; found C 40.27, H 4.67, N 12.38. Cyclic voltammetry (250 mV/s) in DMSO (1 mM): $E_{1/2}$ = −74 mV (Zn^{II}−Fe^{II}/Zn^{II}−Fe^{III}). The cathodic peak at −720 mV is assigned to arsenic, μ_{eff} = 6.06 μ_B.

[$Zn^{II}Fe^{III}$(bdmbbppo)(O_2AsMe_2)](ClO_4)$_2$·5MeOH (3): After the reaction of Hbdmbbppo (103 mg, 0.17 mmol) in methanol (3 mL) with a methanol solution (2.5 mL) of $Zn(ClO_4)_2$·6H_2O (64 mg, 0.17 mmol), a methanol solution (2.5 mL) of $Fe(ClO_4)_3$·H_2O (62 mg, 0.17 mmol) was added dropwise after a few minutes. Finally, the sodium salt of cacodylic acid (38 mg, 0.18 mmol) in methanol (2 mL) was added. Slow evaporation of the solvent yielded brown crystals (41 mg, 0.04 mmol, 24%) suitable for X-ray crystallography. UV/Vis (methanol): λ_{max} = 335 nm (sh) (ε = 2570 $M^{-1}cm^{-1}$). $C_{39.5}H_{55}AsCl_3FeN_8O_{27.5}Zn$ (1224.4): calcd. C 38.75, H 4.53, N 9.15; found C 37.60, H 4.67, N 9.12. Cyclic voltammetry (250 mV/s) in acetonitrile (1 mM): $E_{1/2}$ = 157 mV (Zn^{II}−Fe^{II}/Zn^{II}−Fe^{III}). The cathodic peak at −740 mV is arsenic-centered, μ_{eff} = 6.00 μ_B.

[Zn^{II}_2(tdmbpo)(O_2AsMe_2)(HOMe)](ClO_4)$_3$·4MeOH·2H_2O (4): A methanol solution (5 mL) of $Zn(ClO_4)_2$·6H_2O (128 mg, 0.34 mmol) was added to a suspension of Htdmbpo (141 mg, 0.17 mmol) in methanol (10 mL). Then the sodium salt of cacodylic acid (37 mg, 0.17 mmol), dissolved in methanol (5 mL), was added to the solution. Colorless crystals (74 mg, 0.06 mmol, 35%) were obtained after 2 d by slow evaporation of the solvent. $C_{50}H_{75}AsCl_2N_{10}O_{16}Zn_2$ (1348.8): calcd. C 44.52, H 5.61, N 10.39; found C 43.20, H 5.47, N 10.70.

[Zn^{II}_2(bdmbbppo)(O_2AsMe_2)](ClO_4)$_2$·H_2O (5): An aqueous solution (3 mL) of $Zn(ClO_4)_2$·6H_2O (128 mg, 0.34 mmol) and an aqueous solution (2 mL) of the sodium salt of cacodylic acid were added to a solution of Hbdmbbppo (101 mg, 0.17 mmol) in acetonitrile (5 mL). Diffusion of diethyl ether into the solution afforded colorless crystals (101 mg, 0.09 mmol, 55%) after 4 d. $C_{37}H_{47}AsCl_2N_8O_{12}Zn_2$ (1072.4): calcd. C 41.44, H 4.42, N 10.45; found C 40.27, H 4.55, N 10.14.

pH-Metric Measurements: The protonation and coordination equilibria were investigated by potentiometric titration in an ethanol/water solvent mixture (35 or 80 % ethanol, w/w) [*T* = 298 ± 0.1 K, *I* = 0.1 M and 0.05 M ($NaNO_3$) for 35 and 80 % ethanol/water, w/w mixture, respectively], using an automatic titration set including a Dosimat 665 (Metrohm) autoburette, an Orion 710A precision digital pH-meter and an IBM-compatible PC. 20-mL sample solutions were titrated with 0.1 M NaOH, prepared from solid NaOH (Fluka) in an ethanol/water mixture. The accurate concentration of the NaOH solution was determined by KH−phthalate. The sample solutions were prepared from stock solutions of $Zn(ClO_4)_2$ and the corresponding ligands. The Orion 8103BN semimicro pH glass electrode was calibrated using standard aqueous buffer solutions (pH = 4.0, 7.0 and 10, Sigma) and the actual pH in the mixed solvent was then determined by subtracting 0.10 or 0.11 units (for 35 and 80% ethanol/water, w/w mixture, respectively) from the pH-meter reading according to the method of Bates.[42] The ionization constants of water determined by us under the conditions used [pK_w = 14.53(2) and 15.31(2) for 35 and 80 % ethanol/water, w/w

mixture, respectively] are in good agreement with the literature data.[43] The species formed in the systems were characterized by the general equilibrium process of Equation (1), where M denotes the metal ion and L the nonprotonated (neutral) ligand molecule.

$$pM + qL + rH \xleftrightarrow{\beta_{M_pL_qH_r}} M_pL_qH_r \quad (1)$$

The corresponding formation constants ($\beta_{M_pL_qH_r} \equiv \beta_{pqr} = [M_pL_qH_r]/[M]^p[L]^q[H]^r$) were calculated using the computer program PSEQUAD,[44] as concentration constants. The protonation and complex formation constants were determined from 3 and 6 independent titrations (60−80 data points per titration), respectively. The metal/ligand ratios varied between 1:2 and 3:1, with the metal ion concentration between 1.0×10^{-3} and 2.5×10^{-3} mol·dm^{-3}.

Kinetic Measurements: The transesterification of 2-(hydroxypropyl)-4-nitrophenyl phosphate[40] (hpnp) was monitored in a buffered ethanol/water mixed solvent [I = 0.1 or 0.05 M ($NaNO_3$), T = 298 K] by detecting the increase in the absorbance maximum at 400 nm of the 4-nitrophenolate anion (ε = 18900) (Figure 6). In all cases 0.04 M buffer (HEPES and CHES) was used. The pK of 4-nitrophenol was determined independently for our conditions (pK = 7.50 ± 0.02 and 8.47 ± 0.02 for 35 and 80% ethanol/water mixture, respectively). The initial concentration of hpnp varied from 0.4 mM to 9 mM. The initial slope method (≤ 4% conversion) was used to determine the pseudo-first-order rate constants. The reported data are the average of triplicate measurements with a reproducibility better than 10%. In a typical experiment, the pH of the solution containing 0.4−0.8 mM ligand, 0.8−1.6 mM zinc(II), buffer and background electrolyte was adjusted to the desired value. 2 mL of this solution was equilibrated at 298 K in the spectrophotometer, 100 μL of 0.02 M hpnp was then injected into the solution with efficient mixing. The increase in the absorbance at 400 nm was immediately monitored. Second-order rate constants were obtained from plots of first-order rate constants against the concentration for the complex $Zn_2LH_{-1}(OH)$, calculated from the formation constants determined by pH-metry.

X-ray Data Collection and Crystal Structure Determinations: The unit cell parameters and basic information about data collection and structure refinement are given in Table 6. Structures were solved by heavy-atom methods (SHELXS-97) and refined by full-matrix least-squares methods based on F^2 (SHELXL-97).[45] The location of a half occupied nitrate anion in **2** was not possible due

Table 6. Crystallographic data for **1** to **5**

	1	**2**	**3**	**4**	**5**
Empirical ormula	$C_{50}H_{79}AsCl_3FeN_{10}O_{22}Zn$	$C_{45}H_{63}AsClFeN_{12}O_{21.5}Zn$	$C_{39.5}H_{55}AsCl_3FeN_8O_{17.5}Zn$	$C_{50}H_{75}AsCl_2N_{10}O_{16}Zn_2$	$C_{37}H_{47}AsCl_2N_8O_{12}Zn_2$
Formula mass	1474.72	1347.66	1224.41	1348.76	1072.39
a [Å]	35.239(7)	13.520(3)	11.088(2)	12.278(2)	11.148(2)
b [Å]	13.113(3)	15.172(3)	20.975(4)	14.079(3)	22.546(5)
c [Å]	28.375(6)	16.191(3)	22.636(5)	19.702(4)	18.854(4)
α [°]	90	84.76(3)	90	84.72(3)	90
β [°]	92.85(3)	74.67(3)	99.84(3)	81.41(3)	101.51(3)
γ [°]	90	68.61(3)	90	65.53(3)	90
V [Å^3]	13096(5)	2982.3(10)	5187.0(18)	3063.3(10)	4643.5(17)
Z	8	2	4	2	4
$d_{calcd.}$ [g/cm^3]	1.487	1.466	1.560	1.458	1.531
Crystal system	monoclinic	triclinic	monoclinic	triclinic	monoclinic
Space group	$C2/c$	$P\bar{1}$	$P2_1/c$	$P\bar{1}$	$P2_1/n$
Diffractometer	Smart CCD	Smart CCD	STOE IPDS	Siemens P3	STOE IPDS
Radiation, λ [Å]	Mo-K_α = 0.7107				
Monochromator	graphite plate				
Crystal size [mm]	0.32×0.21×0.17	0.30×0.20×0.19	1.16×0.16×0.16	0.35×0.28×0.23	0.40×0.32×0.10
T [K]	150(2)	150(2)	213(2)	153(2)	213(2)
Scan type, Θ range [°]	ω, 3.66−34.06	ω, 1.30−28.26	, 4.33−26.01	ω, 2.01−27.00	, 4.28−26.12
Index ranges	−48≤h≤42	−17≤h≤17	−12≤h≤13	−4≤h≤10	−13≤h≤13
	−14≤k≤17	−20≤k≤20	−25≤k≤25	−16≤k≤17	−27≤k≤27
	−37≤h≤42	−21≤h≤21	−27≤h≤26	−24≤h≤25	−22≤h≤22
Reflections measured	42187	25157	40449	11443	36688
Number of symmetry-independent reflections	15973	12082	9572	10822	8645
μ [mm^{-1}]	1.291	1.321	1.605	1.478	1.921
Solution	SHELXS-97, patterson method				
LS refinements	SHELXL-97, against F^2				
Refined reflections	15973	12082	9572	10822	8645
Parameters	849	703	719	761	570
GooF on F^2	0.990	1.052	1.051	1.341	1.017
Final $R1$ and $Rw2$ [$I > 2\sigma(I)$]	0.0752/0.1751	0.0821/0.2459	0.0651/0.1615	0.0989/0.2264	0.0977/0.2008
Final $R1$ and $Rw2$ (all data)	0.1519/ 0.2030	0.0896/0.2546	0.0937/0.1797	0.2115/0.2842	0.1699/0.2450
Largest diff. peak and hole	1.583/−0.739	4.338/−0.896	1.232/−0.652	1.649/−3.935	1.260/−0.747

to high remaining electron densities and severe disorder. The charge of the iron center was confirmed by magnetic susceptibility measurements. The nitrate anions, water molecules and one hydroxyethyl group of the ligand in **2** were refined with isotropic thermal parameters. All other non-hydrogen atoms were refined anisotropically, with the exception of the two water molecules in **1**, the disordered carbon atom of the methanol molecule that is coordinated to the iron center in **3**, one carbon atom of the ligand in **4** and a disordered oxygen atom of a perchlorate anion and a water molecule in **5**. Hydrogen atoms were placed in calculated positions and refined with a riding model with U_H(CH, CH_2, NH) = 1.2·U_{eq}(C) and U_H(CH_3, OH) = 1.5·U_{eq}(C) and 1.5·U_{eq}(O), respectively. High *R* values are caused by bad crystal quality. CCDC-169381−169385 contain the supplementary crystallographic data for this paper. These data can be obtained free of charge at www.ccdc.cam.ac.uk/conts/retrieving.html or from the Cambridge Crystallographic Data Centre, 12, Union Road, Cambridge CB2 1EZ, UK [Fax: (internat.) + 44-1223/336-033; E-mail: deposit@ccdc.cam.ac.uk].

Acknowledgments

The authors are grateful to Dr. F. Schweppe, Dr. K. Kirschbaum and Prof. Dr. A. A. Pinkerton for the X-ray crystallographic measurement of complex **1**. S. A., D. S. and B. K. thank the Deutsche Forschungsgemeinschaft and the Fonds der Chemischen Industrie for support. A. J. and T. G. thank the Foundation of Research Development at Universities (FKFP 0190/2000) for financial assistance.

[1] T. Klabunde, N. Sträter, R. Fröhlich, H. Witzel, B. Krebs, *J. Mol. Biol.* **1996**, *259*, 737−748.
[2] J. P. Griffith, J. L. Kim; E. E. Kim, M. D. Sintchak, J. A. Thompson, M. J. Fitzgibbon, M. A. Fleming, P. R. Caron, K. Hsiao, M. A. Navia, *Cell* **1995**, *82*, 507−522.
[3] J. Goldberg, H. Huang, Y. Kwon, P. Greengard, A. C. Nairn, I. Kurivan, *Nature* **1995**, *376*, 745−753.
[4] B. Stec, K. M. Holtz, E. R. Kantrowitz, *J. Mol. Biol.* **2000**, *299*, 1323−1331.
[5] E. Hough, L. K. Hansen, B. Birknes, K. Jynge, S. Hansen, A. Hordvik, C. Little, E. Dodson, Z. Derewenda, *Nature* **1989**, *338*, 357−360.
[6] A. Volbeda, A. Lahm, F. Sakiyama, D. Suck, *EMBO J.* **1991**, *10*, 1607−1618.
[7] J. L. Vanhooke, M. M. Benning, F. M. Raushel, H. M. Holden, *Biochemistry* **1996**, *35*, 6020−6025.
[8] E. E. Kim, H. W. Wyckoff, *J. Mol. Biol.* **1991**, *218*, 449−451.
[9] S. Uhlenbrock, B. Krebs, *Angew. Chem. Int. Ed. Engl.* **1992**, *31*, 1647−1648.
[10] F. Meyer, P. Rutsch, *Chem. Commun.* **1998**, 1037−1038.
[11] C. He, S. J. Lippard, *J. Am. Chem. Soc.* **2000**, *122*, 184−185.
[12] N. W. Kaminskaia, C. He, S. J. Lippard, *Inorg. Chem.* **2000**, *39*, 3365−3373.
[13] Y. Hayashi, T. Kayatani, H. Sugimoto, M. Suzuki, K. Inomata, A. Uehara, Y. Mizutani, T. Kitagawa, Y. Maeda, *J. Am. Chem. Soc.* **1995**, *117*, 11220−11229.
[14] C. Belle, G. Gellon, C. Scheer, J.-L. Pierre, *Tetrahedron Lett.* **1994**, *35*, 7019−7022.
[15] C. Belle, I. Gautier-Luneau, G. Gellon, J.-L. Pierre, I. Morgenstern-Badarau, E. Saint-Aman, *J. Chem. Soc., Dalton Trans.* **1997**, 3543−3546.
[16] C. Belle, J.-L. Pierre, E. Saint-Aman, *New J. Chem.* **1998**, 1399−1402.
[17] C. Belle, I. Gautier-Luneau, J.-L. Pierre, C. Scheer, E. Saint-Aman, *Inorg. Chem.* **1996**, *35*, 3706−3708.
[18] A. Neves, L. M. Rossi, A. Horn, Jr., I. Vencato, A. J. Bortoluzzi, C. Zucco, A. S. Mangrich, *Inorg. Chem. Commun.* **1999**, *2*, 334−337.
[19] E. Bernard, W. Moneta, J. Laugier, S. Chardon-Noblat, A. Deronzier, J.-P. Tuchagues, J.-M. Latour, *Angew. Chem. Int. Ed. Engl.* **1994**, *33*, 887−889.
[20] W. Kanda, W. Moneta, M. Bardet, E. Bernard, N. Debaecker, J. Laugier, A. Bousseksou, S. Chardon-Noblat, J.-M. Latour, *Angew. Chem. Int. Ed. Engl.* **1995**, *34*, 588−590.
[21] L.-H. Yin, P. Cheng, S.-P. Yan, X. Q. Fu, J. Li, D.-Z. Liao, Z.-H. Jiang, *J. Chem. Soc., Dalton Trans.* **2001**, *9*, 1398−1400.
[22] A. S. Borovik, L. Que, Jr., V. Papaefthymiou, E. Münck, L. F. Taylor, O. P. Anderson, *J. Am. Chem. Soc.* **1988**, *110*, 1986−1988.
[23] A. S. Borovik, V. Papaefthymiou, L. T. Taylor, O. P. Anderson, L. Que, Jr., *J. Am. Chem. Soc.* **1989**, *111*, 6183−6195.
[24] M. Ghiladi, C. J. McKenzie, A. Meier, A. K. Powell, J. Ulstrup, S. Wocadlo, *J. Chem. Soc., Dalton Trans.* **1997**, 4011−4018.
[25] K. Schepers, B. Bremer, B. Krebs, G. Henkel, E. Althaus, B. Mosel, W. Müller-Warmuth, *Angew. Chem. Int. Ed. Engl.* **1990**, *29*, 531−533.
[26] S. Albedyhl, M. T. Averbuch-Pouchot, C. Belle, B. Krebs, J.-L. Pierre, E. Saint-Aman, S. Torelli, *Eur. J. Inorg. Chem.* **2001**, 1457−1464.
[27] M. Suzuki, S. Fujinami, F. Hibino, H. Hori, Y. Maeda, A. Uehara, M. Suzuki, *Inorg. Chim. Acta* **1998**, *283*, 124−135.
[28] M. Yashiro, A. Ishikubo, M. Komiyama, *J. Chem. Soc., Chem. Commun.* **1995**, 1793−1794.
[29] M. Yashiro, A. Ishikubo, M. Komiyama, *Chem. Commun.* **1997**, 83−84.
[30] P. Molenveld, S. Kapsabelis, J. F. J. Engbersen, D. N. Reinhoudt, *J. Am. Chem. Soc.* **1997**, *119*, 2948−2949.
[31] P. Molenveld, J. F. J. Engbersen, H. Kooijman, A. L. Spek, D. N. Reinhoudt, *J. Am. Chem. Soc.* **1998**, *120*, 6726−6737.
[32] P. Molenveld, W. M. G. Stikvoort, H. Kooijman, A. L. Spek, J. F. J. Engbersen, D. N. Reinhoudt, *J. Org. Chem.* **1999**, *11*, 3896−3906.
[33] P. Molenveld, J. F. J. Engbersen, D. N. Reinhoudt, *Eur. J. Org. Chem.* **1999**, 3269−3275.
[34] T. Gajda, R. Krämer, A. Jancsó, *Eur. J. Inorg. Chem.* **2000**, 1635−1644.
[35] A. Jancsó, T. Gajda, E. Mulliez, L. Korecz, *J. Chem. Soc., Dalton Trans.* **2000**, 2679−2684.
[36] C. Duboc-Toia, S. Ménage, J.-M. Vincent, M. T. Averbuch-Pouchot, M. Fontecave, *Inorg. Chem.* **1997**, *27*, 6148−6149.
[37] R. Than, A. Schroft, L. Westerheide, R. van Eldik, B. Krebs, *Eur. J. Inorg. Chem.* **1999**, 1537−1543.
[38] B. Eulering, F. Ahlers, F. Zippel, M. Schmidt, H.-F. Nolting, B. Krebs, *J. Chem. Soc., Chem. Commun.* **1995**, 1305−1307.
[39] B. Eulering, M. Schmidt, U. Pinkernell, U. Karst, B. Krebs, *Angew. Chem. Int. Ed. Engl.* **1996**, *35*, 1973−1974.
[40] D. M. Brown, D. A. Usher, *J. Chem. Soc.* **1965**, 6558−6565.
[41] L. Westerheide, F. K. Müller, R. Than, B. Krebs, *Inorg. Chem.* **2001**, *8*, 1951−1961.
[42] R. G. Bates, *Determination of pH*, 2nd ed., John Wiley & Sons, New York, **1964**, p. 226−227.
[43] E. M. Wooley, D. G. Hurkot, L. G. Hepler, *J. Phys. Chem.* **1970**, *74*, 3908−3916.
[44] L. Zékány, I. Nagypál "PSEQUAD: A Comprehensive Program for the Evaluation of Potentiometric and/or Spectrophotometric Equilibrium Data Using Analytical Derivatives" in *Comptutational Methods for the Determination of Formation Constants* (Ed.: D. J. Leggett), Plenum Press, New York, **1991**.
[45] G. M. Sheldrick, *SHELXS-97, Program for the Solution and Refinement of Crystal Structures*, University of Göttingen, Germany, **1997**.

Received August 28, 2001
[I01334]